Studying the Effect of Cracks on the Ultrasonic Wave Propagation in a Two Dimensional Gearbox Finite Element Model

Didem Ozevin[1], Hossein Fazel[1], Justin Cox[2], William Hardman[2], Seth S Kessler[3] and Alan Timmons[2]

[1]Civil and Materials Engineering, University of Illinois at Chicago, Chicago IL

[2]Naval Air Systems Command, NAS Patuxent River MD

[3]Metis Design Corporation, Boston MA

ABSTRACT:

Gearbox components of aerospace structures are typically made of brittle materials with high fracture toughness, but susceptible to fatigue failure due to continuous cyclic loading. Structural Health Monitoring (SHM) methods are used to monitor the crack growth in gearbox components. Damage detection methodologies developed in laboratory-scale experiments may not represent the actual gearbox structural configuration, and are usually not applicable to real application as the vibration and wave properties depend on the material, structural layers and thicknesses. Also, the sensor types and locations are key factors for frequency content of ultrasonic waves, which are essential features for pattern recognition algorithm development in noisy environments. Therefore, a deterministic damage detection methodology that considers all the variables influencing the waveform signature should be considered in the preliminary computation before any experimental test matrix. In order to achieve this goal, we developed two dimensional finite element models of a gearbox cross section from front view and shaft section. The cross section model consists of steel revolving teeth, a thin layer of oil, and retention plate. An ultrasonic wave up to 1 MHz frequency is generated, and waveform histories along the gearbox are recorded. The received waveforms under pristine and cracked conditions are compared in order to analyze the crack influence on the wave propagation in gearbox, which can be utilized by both active and passive SHM methods.

Keywords: gearbox, crack growth, numerical model.

1. INTRODUCTION

Current Structural Health Monitoring (SHM) methods for real time damage detection in gearbox components are mostly based on experimental and historical data. The experiments are typically conducted at laboratory scale tests at controlled environment using artificially introduced defects. Gearboxes are prone to develop local cracks and spalling defects due to excessive loads, insufficient lubricants, manufacturing defects, installation problems or material fatigue. The most common SHM methods for gearbox damage monitoring in laboratory scale tests include acoustic emission [1, 2, 3] and vibration [4] while the vibration method is also implemented in field tests. For the acoustic emission (AE) method, active flaws generate wide-band sources propagating through the complex geometries and interfaces of gearbox and reaching to the sensors mounted on the gearbox housing. The presence of splines adds additional interface to the propagating path

(splines indicate area contact while gears indicate point/line contact). The method relies on searching for the presence of high frequency waves as compared to extraneous noise emissions, which are typically dominated by low frequency signals. For the vibration method, the progression of damage is extracted from time and frequency domain features of low frequency vibration data recorded by accelerometers in order to assess the changes in vibrational properties in time as related to the damage. There are several approaches to combine two methods for redundant measurement. Ozevin et al. [5] implemented the combined acoustic emission/vibration sensors in the same package for concurrent data collection from gearbox components. Loutas et al. [6] combined vibration, acoustic emission and oil-debris monitoring methods for a more effective condition monitoring approach for rotating machinery. The authors applied principal component analysis (PCA) to reduce the number of parameters extracted from three methods, and concluded that the AE method is not sensitive to gear wear while the method detects the tooth crack earlier than the vibration monitoring. Typical parameters extracted from the waveforms of AE and vibration data are root mean square value, spectral kurtosis, peak-to-peak vibration level, and ratio of the amplitude of the second tooth-meshing frequency. There are also advanced signal processing approaches such as wavelet decomposition of time domain data instead of traditional time domain features [7]. Le and He [8] applied empirical mode decomposition to the AE data for quantifying damage in gearbox. The relations between damage and parameters are built based on the experimental data. For instance, Sentoku [9] concluded that the AE amplitude and energy increased with increased pitting using the AE sensor mounted on the gear wheel. However, variations in components (e.g., lubrication level, installation method), environmental factors (e.g., temperature, operational condition) and loads (e.g. excessive torque) may influence the time and frequency domain features, and cause the development of universal damage algorithm difficult.

Numerical methods have the ability to study the static and dynamic behaviors of complex structural systems. Gearbox systems have a multi-layer structure with different materials; therefore, there is no close-form solution to understand their behavior. There are many studies to understand the variations in dynamic properties of gearboxes for the vibration monitoring [e.g., 10, 11, 12]. The numerical models provide variations in the gear-mesh stiffness due to the presence of the defect. However, the gear-mesh stiffness may vary depending on the tooth geometry, the position of the contact point, gear tooth deflections, gear tooth profile errors and gear hub torsional deformation in addition to the local faults on the tooth [13].

Table 1 – Summary of common methods for monitoring damage at gearbox components

Method	**Advantage**	**Disadvantage**
Acoustic Emission	High frequency method, sensitive to small cracks	The method requires intense experimental design, signal attenuation, and high background noise influences the data set negatively
Vibration	Well-established, accurate calculation of gear mesh stiffness	Insufficient sensitivity to small cracks, potential influence of gearbox operational condition
Debris Monitoring	No need for electronics, simple interpretation, excellent sensitivity to spalling failure	Insufficient sensitivity to non-benign cracks as no debris is produced

While passive SHM methods provide real time damage detection possibility, they suffer from varying conditions of gearbox operation as discussed above. Table 1 summarizes the advantages and disadvantages of three common damage monitoring methods for the gearbox structure. A method independent from gearbox operations is needed. In this study, active ultrasonic method is explored as a new alternative to passive SHM methods for damage detection at spline teeth. Numerical simulations of wave propagation through spline cross section up to 1 MHz excitation frequency are studied.

The purpose of numerical simulations is to implement the ultrasonic method for monitoring the damage state of spline at frequent intervals as the first time in literature. The approach is independent from the operational conditions of the gearbox as the ultrasonic measurements will be taken when the gearbox is not operational while the method does not require dis-assembly of gearbox because of permanent installation of piezoelectric wafer sensors around the gear section. The waveforms recorded from pristine and cracked conditions are studied.

The organization of this paper is as follows. The numerical models are described in section 2. The mesh optimization to reach accurate model with reasonable computation time are presented in section 3. Section 4 presents the numerical results. Finally, the discussion and conclusions are presented in section 5.

2. DESCRIPTION OF NUMERICAL MODEL

Studying high frequency wave propagation requires very fine meshing and small time step in order to reach numerically accurate solution and prevent numerical pollutions, which may cause spurious waves, incorrect wave amplitudes and arrival times. Therefore, 3D model is practically not possible for dynamic simulations. In this study, the gearbox is divided into two cross sections in order to study the wave propagation at pristine and cracked sections, Figure 1. The front section, Figure 1a, includes gear (steel), retention plate (titanium) and thin oil layer between gear and retention plate; the side section, Figure 1b, considers only the gear detail along the gearbox axis. The mesh size was set as 1/20th of minimum wavelength, which was calculated using 5000 m/s wave velocity. The time step was set as 1/20th of the inverse of the target frequency.

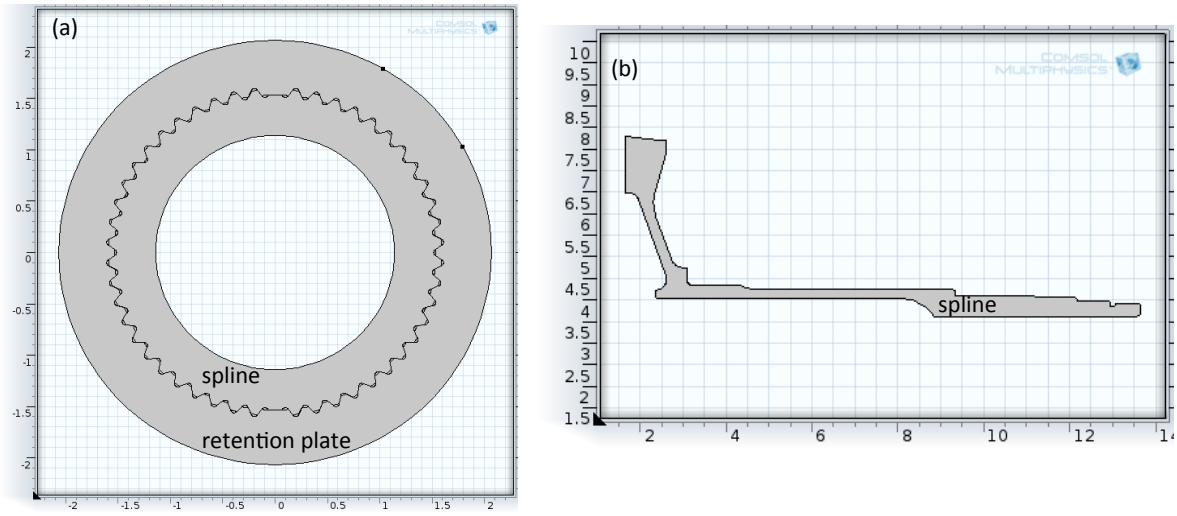

Figure 1. The geometries of numerical models; (a) front section, (b) side section

The excitation signal was defined as four-cycle Hanning window using the following equation:

$$f(t) = \sin(2\pi f t)\frac{1}{2}\left[1 - \cos\left(2\pi\frac{n}{N-1}\right)\right] \quad (1)$$

where f is frequency, n is number of cycles, N is total number of points representing the waveform. The excitation frequency was varied in order to understand their sensitivities to the crack width and length. The excitation signal was applied to the horizontal axis on the surface of the retention plate for the front section model, and the mid-plane at the right-end of the gear for the side section model.

The time histories along the circumference of retention plate for the front section model (for the purpose of through-transmission approach), and at the excitation point for the side section model (for the purpose of pulse-echo approach) were recorded for pristine and cracked conditions. A crack with half tooth width and 0.001 inch wide is introduced to a tooth as the initial model, Figure 2. This crack model is similar to Chaari [13]. The crack length was modified gradually for the parametric study. The influence of the relative position of measurement point to the crack location was studied. The preliminary front section model has the idealized tooth design as the curved structures cause significant increase in mesh density, and computational time. In the actual state of gearbox operation, only one side of spline teeth is in contact with the retention plate. However, small gap between teeth would also cause significant mesh density at the narrow gap, both sides of spline tooth were brought in contact with the retention plate. Two physical models of structural and acoustics were coupled. The retention plate and gear were modeled as structural model while the fluid between two layers was modeled as acoustic model as shear wave does not exist in fluid. All the boundaries were defined as natural boundary conditions.

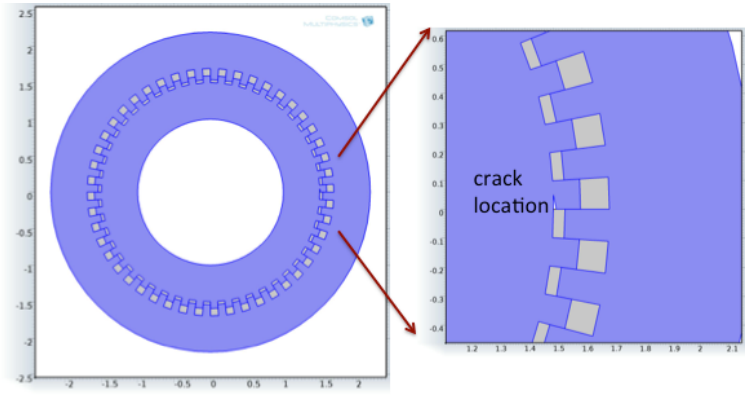

Figure 2. The cracked section geometry for the front section model

3. MESH OPTIMIZATION

The mesh density and element type are essential for accurate modeling of high frequency wave propagation problem. As discussed above, the prevention of numerical pollution requires about $1/20^{th}$ of minimum wavelength expected. Figure 3 and Figure 4 show the images of mesh density, loading shape and loading location for the front and side section models, respectively. The front section model includes a tooth crack, clearly seen at the location of the increased mesh density. The loading was applied to the horizontal line on the retention plate. The bottom-right figure shows the total surface displacement at the initiation of the loading.

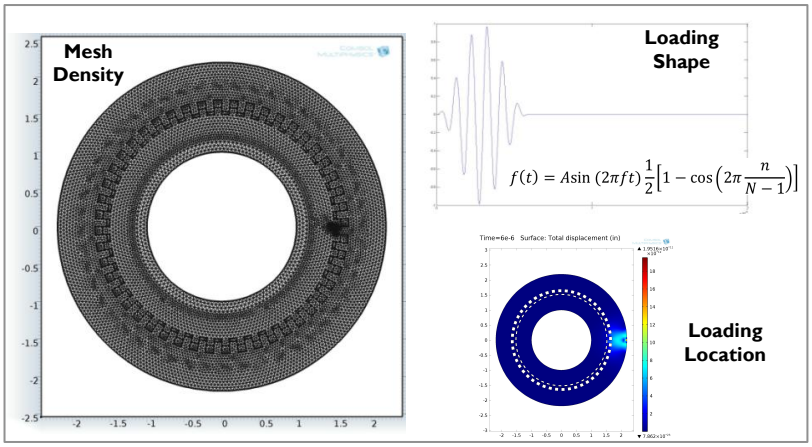

Figure 3. The images of mesh density, loading shape and loading location for the front section model

For the case of the side section model, Figure 4, the input excitation or loading was introduced to the mid-plane of the right-end boundary.

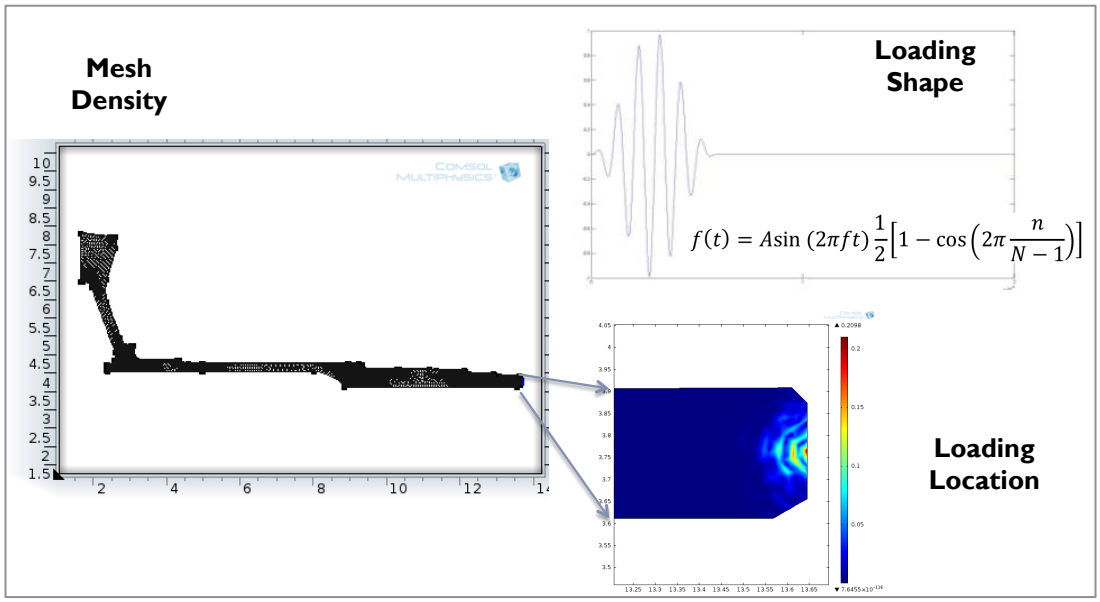

Figure 4. The images of mesh density, loading shape and loading location for the side section model

In order to determine the maximum mesh size, the front section model was computed under three different mesh sizes using various wave velocities and λ/mesh ratios for the 200 kHz excitation signal. The selected maximum mesh sizes are 2.5 mm (referred as mesh 1 using 5000 m/sec wave velocity and λ/mesh as 10), 1.25 mm (referred as mesh 2 using 5000 m/sec wave velocity and λ/mesh as 20), and 0.75 mm (referred as mesh 3 using 3000 m/sec wave velocity and λ/mesh as 20). Figure 5 shows the displacement histories at the top surface of the retention plate at horizontal direction. The amplitudes of mesh 1 and mesh 2 are different; additionally, larger mesh size distorts the wave causing phase difference. The phase difference occurs because of incorrect mesh velocity. The mesh does not move with the actual wave velocity. The comparison of mesh 2 and mesh 3 reveals that the maximum mesh size can be determined using 5000 m/sec wave velocity, and λ/mesh as 20.

Using the pre-determined maximum mesh size, the front section model was run for 100 kHz and 200 kHz excitation signals, and the side section model was run for 500 kHz and 1MHz excitation signals under pristine and cracked conditions. The results are discussed in the following section.

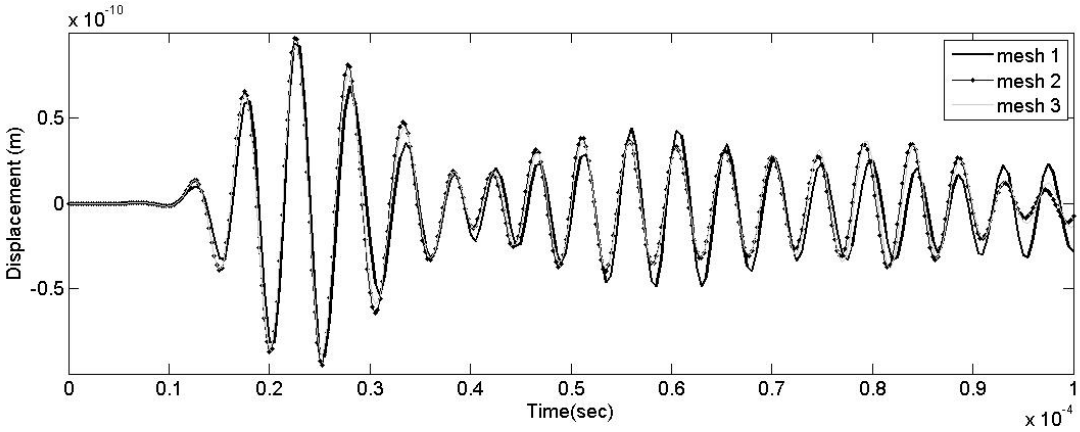

Figure 5. The comparison of displacement histories at the top surface of the retention plate using three different mesh sizes

4. NUMERICAL RESULTS

In this section, the numerical simulation results of the front and side sections of the gearbox are presented under the pristine and cracked conditions. The excitation frequency is varied to understand the frequency sensitivity to the crack size.

4.1. 2D Model of the Front Section

The front section model was simulated under two excitation frequencies: 100 kHz and 200 kHz. The comparison of displacement histories under no crack, 0.05 inch crack and 0.1 inch crack lengths for the 100 kHz excitation signal is shown in Figure 6. There is no difference between the pristine condition and the cracked condition up to 0.1 inch crack length, which implies that the 100 kHz wave is not sensitive to the present crack size.

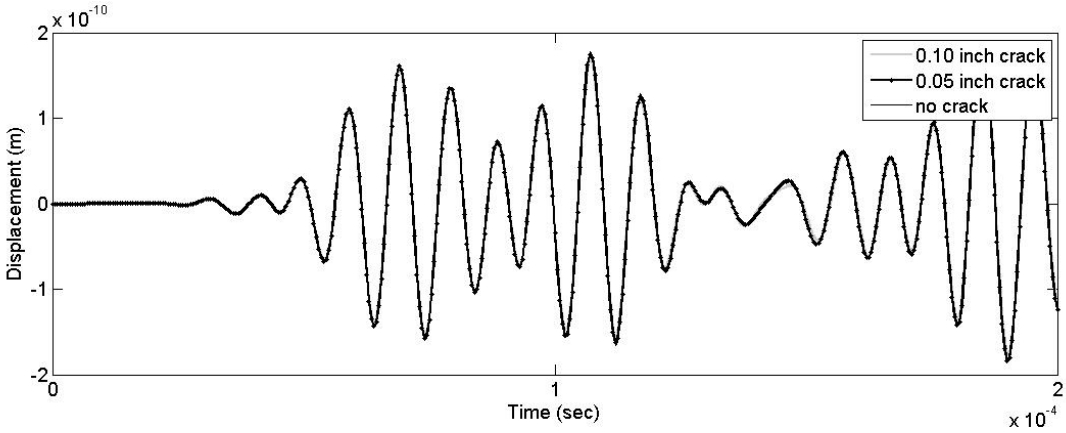

Figure 6. The displacement histories at the top surface of the retention plate for three different crack sizes under 100 kHz excitation signal

As the excitation signal of 100 kHz is not sensitive to the presence of crack, the input signal frequency is increased to 200 kHz. Figure 7 shows the comparison of pristine condition (no crack) and 0.05 inch long crack. The first two wave envelopes have the same characteristics; however, after about 120 μs, a phase different between two signals is observed, which may occur due to scatter from the crack tip.

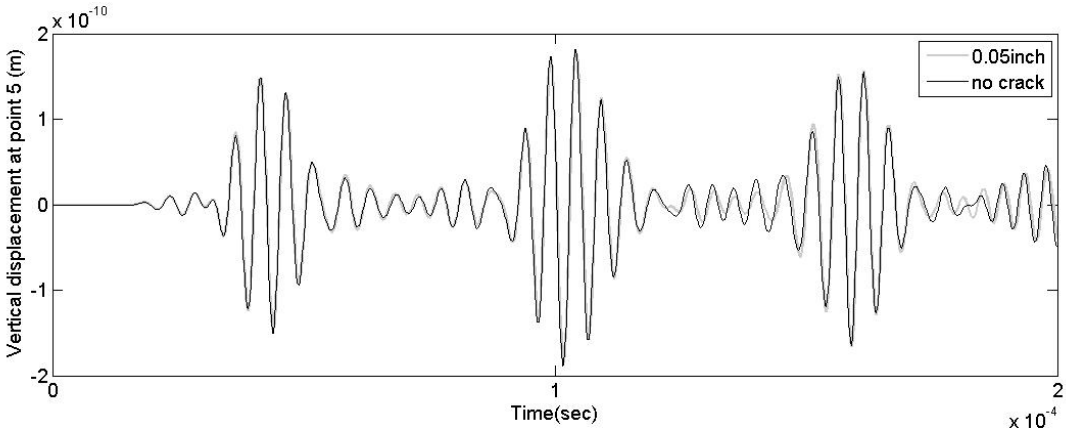

Figure 7. The displacement histories at the top surface of the retention plate (point 5) for no crack condition and 0.05 inch crack length under 200 kHz excitation signal

When the crack length is increased to 0.1 inch, Figure 8, the influence of the crack on propagating waves is clearly observed after the first wave envelope, which propagates through the surface of retention plate without any interaction with crack. After the 60 μs propagation time, the phase and magnitude of waveform vary due to the presence of crack. However, the phase influence is more apparent than the magnitude change. Therefore, the damage index in frequency domain should be applied to the windowed signal selected after 60 μs.

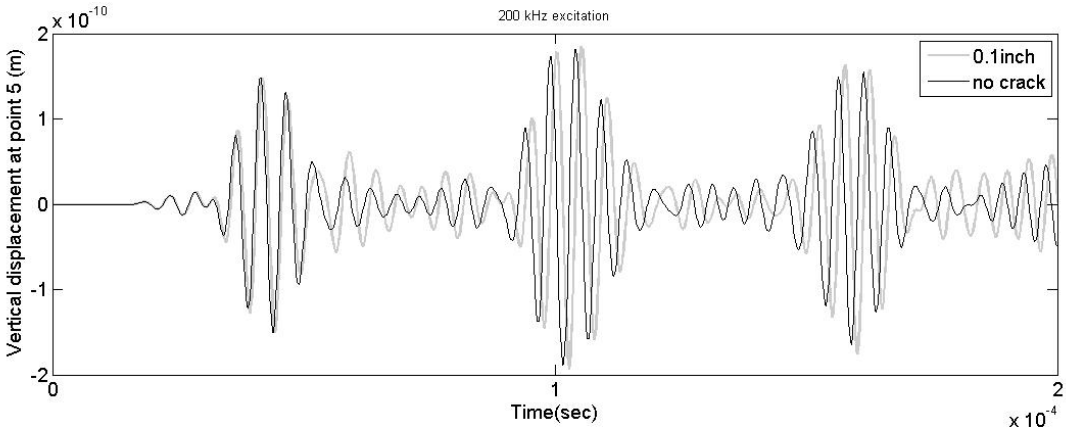

Figure 8. The displacement histories at the top surface of the retention plate for no crack condition and 0.1inch crack length under 200 kHz excitation signal

4.2. 2D Model of the Side Section

The side section model under pristine and cracked conditions was run under the excitation frequencies of 500 kHz and 1MHz. The crack was introduced about two inches away from the right end of the shaft, Figure 9. The crack width and length were defined as 0.001 inch and 5/32 inch, respectively. The figure also shows the mesh density with 1/20th of wavelength resolution for 5000 m/s wave velocity and 500 kHz frequency.

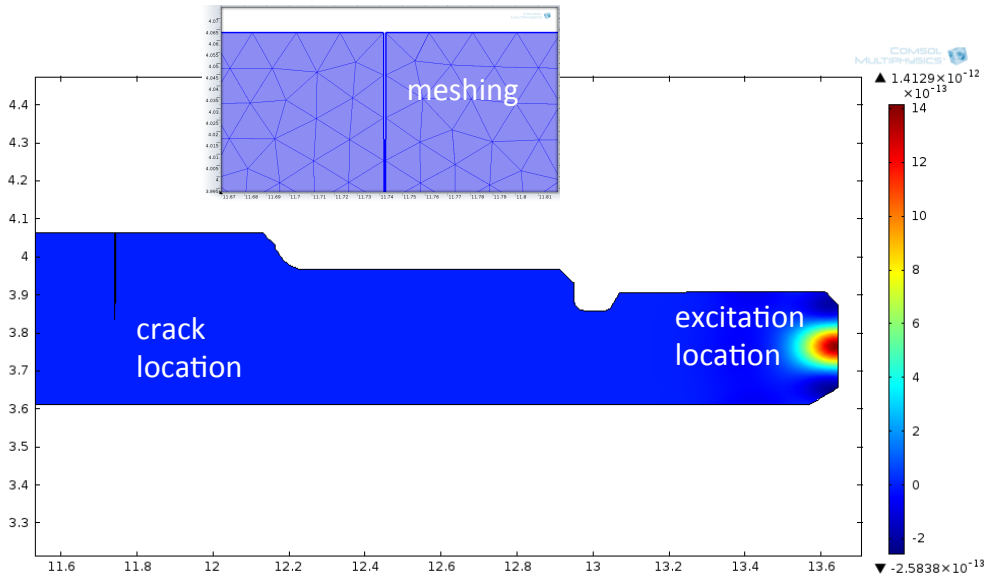

Figure 9. The crack location and mesh around crack for the side section model

The implicit time integration was performed every 0.1 μs up to 100 μs. The estimated wave arrival due to the reflection from the crack surface to the excitation location is 40 μs. The images of total displacement responses at three selected time points as 2 μs, 10 μs and 20 μs are shown in Figure 10 for the uncracked and cracked conditions for the 500 kHz excitation signal. The images at 2 μs and 10 μs for the uncracked and cracked conditions are the same. When the wave field reaches to the crack front, it is distorted causing wave reflections and scatters, which modify the value of total displacement magnitude along the gear section as shown in the image of 20 μs.

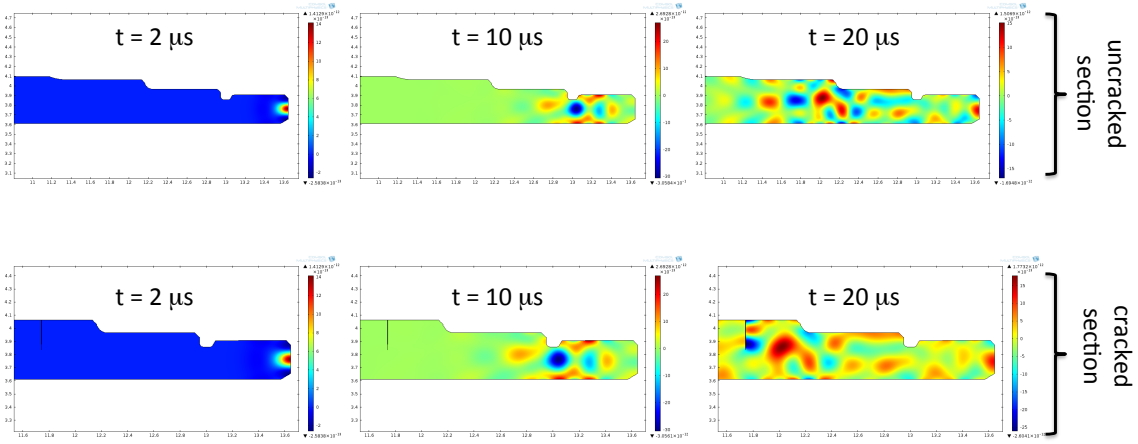

Figure 10. The total displacement response at four selected time points for the 500 kHz excitation

The horizontal displacement histories at the excitation point for the 500 kHz and 1 MHz excitation signals are shown in Figure 11 and Figure 12, respectively. The simulation of the 1 MHz excitation frequency was performed till 50 μs. The reflected wave from the crack tip is observed near 40 μs for both simulations. The ratios of transmitted wave amplitude to the reflected wave amplitude for the 500 kHz and 1 MHz excitation signals are about six and eight, respectively. Low frequency excitation has stronger reflection component due to smaller attenuation factor; however, it may lose sensitivity to smaller crack size.

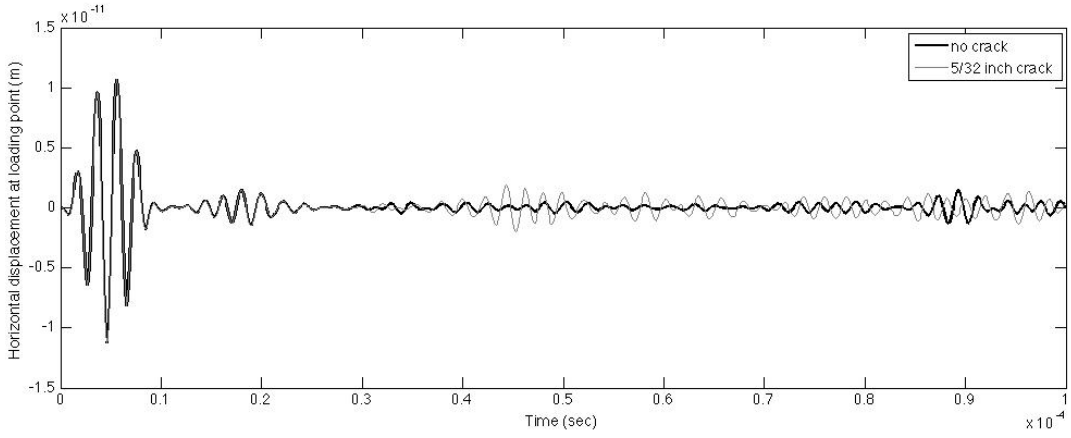

Figure 11. The horizontal displacement histories at the loading point for the pristine and cracked conditions of the side model for the 500 kHz excitation

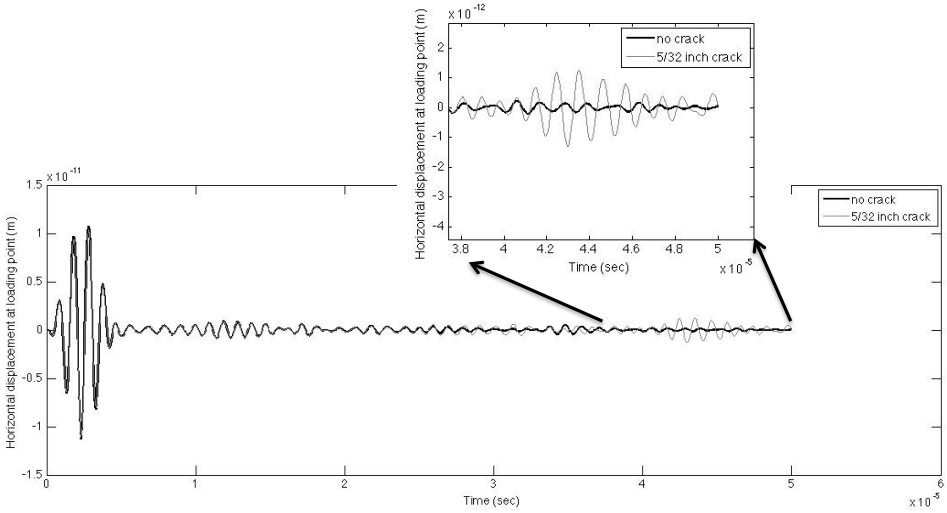

Figure 12. The horizontal displacement histories at the loading point for the pristine and cracked conditions of the side model for the 1MHz excitation

5. CONCLUSIONS

In this paper, propagation of high frequency signals at pristine and cracked sections of gearbox is studied. The gearbox model is divided into the front section and the side section models in order to reduce the computational time. The mesh optimization study revealed that the maximum mesh density can be set using $1/20^{th}$ of wavelength using 5000 m/s wave velocity for each particular frequency resolution. The front section model shows that the minimum frequency should be set as 200 kHz to detect crack size less than 0.1 inch. The side section model is simulated up to 1 MHz for the purpose of pulse-echo approach where the sensors are mounted at the mid-plane of right-end side of gear. The wave reflections from the crack surface are observed after 40 μs. Therefore, damage indexes should be applied within the time window of 40-50 μs. The numerical simulations show that the active ultrasonic method is an alternative to conventional passive SHM methods including AE and vibration while the approach may tackle the challenge of operational dependent response of the passive methods. The future work of this study includes extending 2D finite element model to 3D quadratic model, and validating the numerical results with experiments.

6. ACKNOWLEDGMENTS

This material is based upon work supported by the U.S. Naval Air Systems Command (NAVAIR) under Contract No. N68335-13-C-0417 entitled "Hybrid State-Detection System for Gearbox Components" awarded to the Metis Design Corporation. Any opinions, findings and conclusions or recommendations expressed in this material are those of the authors and do not necessarily reflect the views of NAVAIR.

7. REFERENCES

1 B. Eftekharnejad and D. Mba. “Monitoring Natural Pitting Progress on Helical Gear Mesh using Acoustic Emission and Vibration,” Strain, Vol. 47, pp. 299-310 (2011).

2 B. Eftekharnejad, A. Addali, D. Mba, “Shaft Crack Diagnostics in a Gearbox,” Applied Acoustics, Vol. 73, pp. 723-733 (2012).

3 R. Li, S.U. Seckiner, D. He, E. Bechhoefer, and P. Menon. “Gear Fault Location Detection for Split Torque Gearbox using AE Sensors,” IEEE Transactions on Systems, Man and Cybernetics – Part C: Applications and Reviews, Vol. 42, No. 6, pp. 1308-1317 (2012)

4 I. Yesilyurt, F. Gu and A.D. Ball. “Gear Tooth Stiffness Reduction Measurement using Modal Analysis and its use in

Wear Fault Severity Assessment of Spur Gears," NDT&E International, Vol. 36, pp. 357-372 (2003).

5 D. Ozevin, V. Godinez, J. Dong, and M. Carlos. "Damage Assessment of Gearbox Operating High Noisy Environment Using Waveform Streaming Approach," Journal of Acoustic Emission, pp. 355-363 (2007).

6 T.H. Loutas, D. Roulias, E. Pauly, and V. Kostopoulos, "The Combined use of Vibration, Acoustic Emission and Oil Debris on-line Monitoring towards a more Effective Condition Monitoring of Rotating Machinery," Mechanical Systems and Signal Processing, Vol. 25, pp. 1339-1352 (2011).

7 D.S. Gu, J.G. Kim, Y.S. An, and B.K. Choi. "Detection of Faults in Gearboxes using Acoustic Emission Signal," Journal of Mechanical Science and Technology, Vol. 25, No. 5, pp. 1279-1286 (2011).

8 R. Li and D. He. "Rotational Machine Health Monitoring and Fault Detection using EMD-Based Acoustic Emission Fature Quantification," IEEE Transactions on Instrumentation and Measurement, Vol. 61, No. 4, pp. 990-1001 (2012).

9 H. Sentoku. "AE in Tooth Surface Failure Process of Spur Gear," Journal of Acoustic Emission, Vol. 16 (1-4) S19-S24 (1998).

10 V.G. Sfakiotakis and N.K. Anifantis. "Finite Element Modeling of Spur Gearing Fractures," Finite Elements in Analysis and Design," Vol. 39, pp. 79-92 (2002).

11 Fakher C, Walid B, Mohamed SA, Mohamed H. Effect of spalling or tooth breakage on gearmesh stiffness and dynamic response of a one-stage spur gear transmission. Eur J Mech A-Solid 2008;27:691–705.

12 R. Ma, Y. Chen. "Research on the Dynamic Mechanism of the Gear System with Local Crack and Spalling Failure," Engineering Failure Analysis, Vol. 26, pp. 12-20 (2012).

13 Chaari, F., Fakhfakh, T., and Haddar, M. (2009). "Analytical modeling of spur gear tooth crack and influence on gearmesh stiffness," European Journal of Mecahnics A/Solids, Vo;. 28, pp. 461-468.